Influences of soldering time on wettability and intermetallic phase between Sn-3.0Cu solder and copper substrate

Niwat Mookam and *Kannachai* Kanlayasiri*

Industrial Engineering Department, Faculty of Engineering, King Mongkut's Institute of Technology Ladkrabang, Bangkok, Thailand

Abstract. In this paper, the influences of soldering time on the wettability and intermetallic phase between Sn-3.0Cu lead-free solder and copper substrate were investigated. Reflow soldering was performed at 350 ° C under variable soldering times of 10, 20, 40, 60, 120, 240 and 480 s. The results indicated that the wettability and intermetallic growth depend on the soldering time. In addition, the Cu_6Sn_5 and Cu_3Sn intermetallic phases with a hexagonal crystal structure were found between the lead-free solder and the copper substrate. The growth of intermetallic phases increased with soldering time, and the growth of intermetallic phases remarkably depended on grain boundary diffusion and was volume diffusion-controlled for Cu_6Sn_5 and Cu_3Sn, respectively.

1 Introduction

In the electronic packaging field there is a commitment to quality, and the continuous improvement in developing electronic products also extends to protecting the environment. This often involve which prohibits the use of lead in electronic parts, highlights the requirement of lead-free solder alloys [1]. With the various lead-free solders, Sn-Cu alloy is exposed to the best providing excellent mechanical properties and low cost. Normally, the high-temperature solders are widely used within automotive and energy production industries [2-3]. Sn-3.0Cu alloy is lead-free solder within the high-temperature family suitable for electronics devices.

In the soldering process, a molten solder was contacts with a solid substrate resulting in wetting of the substrate surface. This physical spreading of the solder has several interrelated phenomena such as surface energy, surface tension reduction, interfacial, and chemical reactions [4, 5]. A review of literature also revealed the relationship between the wettability and intermetallic phase formation. The intermetallic phase formation of the interface provides strong wettability [6]. The faster formation rate of intermetallic phase at the interface zone can explain the shorter wetting time [7]. In the work of Wang et al. [8], reported that the intermetallic phase formation can supply driving force for wettability because of the energy relaxation at the interface zone, which promotes the wettability of the solder. However, the phase transformation from Cu_6Sn_5 to Cu_3Sn is a process to discharge energy, which may lead to the increase of the wettability due to the surface tensions of the liquid solder changes according to the change of intermetallic compound (IMC) in the soldering process [9]. Arenas and Acoff [10] reported that the correlation between the intermetallic formation and wettability was no explicit interpretation. Thus, limitation of both prior studies has not been shown relationship of wetting and formation of intermetallic phase, especially with Sn-3.0Cu solder.

This current research investigates the influences of the soldering time on the wettability in term contact angle and the intermetallic phase between Sn-3.0Cu solder and copper substrate. Reflow soldering was then carried out at 350° C under variable soldering times of 10, 20, 40, 60, 120 and 480 s.

2 Experiment

High-temperature Sn-3.0Cu lead-free solder was used in this research. The solidus and liquidus temperatures of this solder are 227 and 309°C, respectively. The solder bar was formed into a cylindrical shape with a diameter of 6.5 mm and thickness of 1.24 mm in accordance with JIS Z3198-3. The substrate was pure copper (99.99%, grade C1100), according to the JIS H3100 standard with thickness 0.2 mm and cut to 25x 30 mm. A confocal laser scanning microscope (CLMS, OLYMPUS, OLS5000) was used to examine microstructures and surface roughness. Substrate grain size was measured following the line-intercept method using OLYMPUS Stream software. The copper surface was cleaned in an HCl solution before fluxing the copper substrate with RC-15SH RMA (15%). A reflow soldering process was followed throughout this research. Copper foil and cylindrical solder rods were soldered using a hot plate at 350°C for times of 10s-480s. After the soldering process, samples were rinsed with ethanol to remove the flux. Wettability of the solders on the foil sheet was tested as the expression of contact angle. Optical microscopy (OM, OLYMPUS, BX 53) was employed to examine the shape of liquid solder spreading over the solid substrate and the contact angle was determined using OLYMPUS Stream software. Microstructure of each specimen after reflow soldering was cut and mounted. Specimens were polished using an argon (Ar) ion beam (IBM, HITACHI, IM 4000

* Corresponding author: kkkannac@kmitl.ac.th

PLUS). Scanning electron microscopy (SEM, JEOL, JSM-5800LV) was then used to verify the microstructure and intermetallic phases, followed by energy dispersive spectroscopy (EDS, OXFORD INSTRUMENTS, X-Max) to determine chemical compositions of the intermetallic phases. SEM images obtained were used to measure the thickness of the intermetallic phases. X-ray diffraction (XRD, Bruker, D8-Discover) was also carried out to analyze the intermetallic compound structures.

3 Results and discussion

3.1 Wettability and contact angle of solder

Surface characteristics and microstructure of the copper substrate play a major role regarding wetting behavior of molten solder. A rough substrate surface improves the wettability in terms of contact angle [11-12]. In addition, grain size (i.e. grain boundary) affects the wetting behavior of molten solder on the substrate. Atomic migrations occur more easily at grain boundaries and increase the free energy of the system which may lead to an increase in wetting kinetics [13]. Fig. 1. demonstrates surface microstructure of the copper substrate before soldering. To examine the grain size number of copper, intercept counting via the test pattern was conducted.

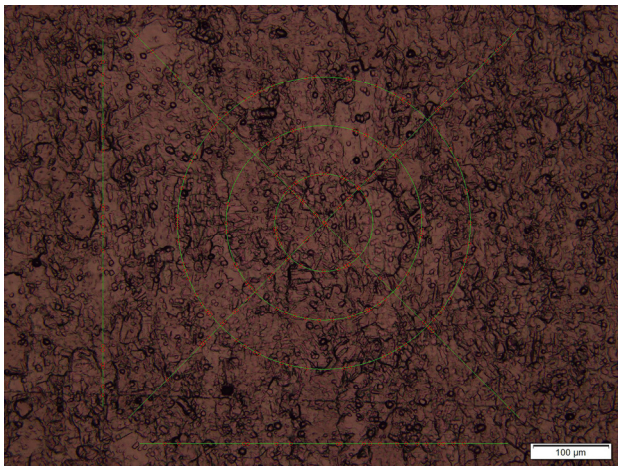

Fig. 1. Surface microstructure of copper substrate.

The grain size number based on the ASTM E112-10 standard was calculated using Equation (1). The original copper substrate exhibited a grain size number of 8.36 for the surface microstructure and was classified as fine grain structure.

$$G = (6.643856 \log \overline{N_L}) - 3.288 \quad (1)$$

Where G is the grain size number and $\overline{N_L}$ is the number of grain intersections per unit length.

Surface roughness was measured at the center of the copper substrate. Surface area was 258.571 µm x 257 µm. Regarding orientation (or direction) analysis, a single-direction was present in the copper substrate due to the rolling process. Examination length was 258.571 µm with arithmetic mean roughness obtained for the copper substrate at 0.165 µm. After soldering, liquid solder in contact with copper in a solid state is depicted in 2D and 3D as a solder joint in Fig. 2. Contact angle of the solder at different soldering times is shown in Fig. 3. Results indicated that the contact angle decreased with reflow time. Zang et al. [14] defined "good wettability" as a contact angle less than 40° and a contact angle between 40 and 50° as "fair wettability". Average contact angles were in the range 8.26°-30.35° and exhibited good wetting behavior of the solder with soldering times ranging from 20s to 240s. In addition, fair wettability was achieved at less than 10s soldering time with contact angle of 48.83°.

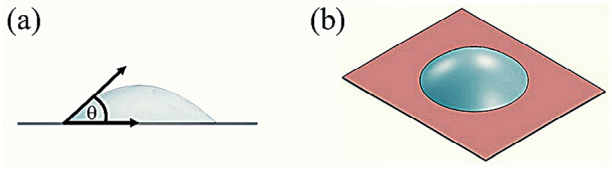

Fig. 2. Schematic of a solder joint; (a) 2D and (b) 3D.

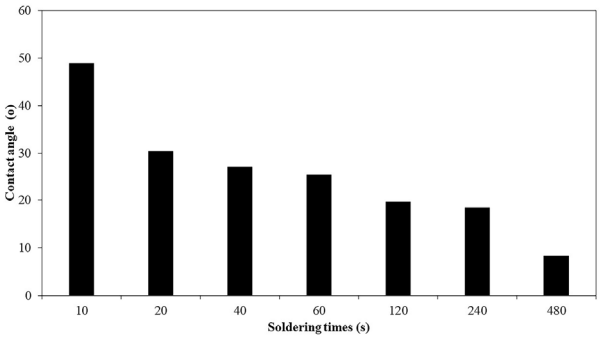

Fig. 3. Contact angle of solder at different soldering times.

3.2 Intermetallic phases

The microstructure and thickness plot of intermetallic phases at different soldering conditions was also examined, as demonstrated in Figures 4 and 5, respectively. To observe the grains of the copper substrate effectively, microstructures were viewed with low magnification and thickness of the intermetallic phases was measured using high magnification. For a given copper substrate, no significant change in grain size of copper substrate was found as soldering time increased. The metal phases found in this experiment were Cu_6Sn_5 and Cu_3Sn. Under soldering conditions of 240s and 480s, a Cu_3Sn phase formed between the copper substrate and the Cu_6Sn_5 phase ($Cu/Cu_3Sn/Cu_6Sn_5$). Generally, increasing thickness of Cu_6Sn_5 was observed with time. This thickness reduced at 240s, with transformation of Cu_6Sn_5 to the Cu_3Sn phase by depletion of Sn which diffused to the Cu side to form a thin phase of Cu_3Sn. In addition, Cu_6Sn_5 phase growth was restricted by the Cu_3Sn phase as fewer Cu atoms diffused from the substrate to the Cu_6Sn_5 phase [15]. After soldering time of 480s, both Cu_6Sn_5 and Cu_3Sn phases showed high growth rates. This occurred as a result of either adding Cu or subtracting Sn from Cu_6Sn_5. Meanwhile, addition of Cu

by Cu atom refers to the dissolved substrate [16-17]. Therefore, Cu_3Sn phase grows rapidly. Elemental compositions of Cu_6Sn_5 and Cu_3Sn were determined by EDS analysis as illustrated in Table 1, and results were consistent with Zuozhu et al. [18]. Crystal structure of the intermetallic phases was hexagonal. The intermetallic phases found in this study were in good agreement with those reported in previous literature [19-20].

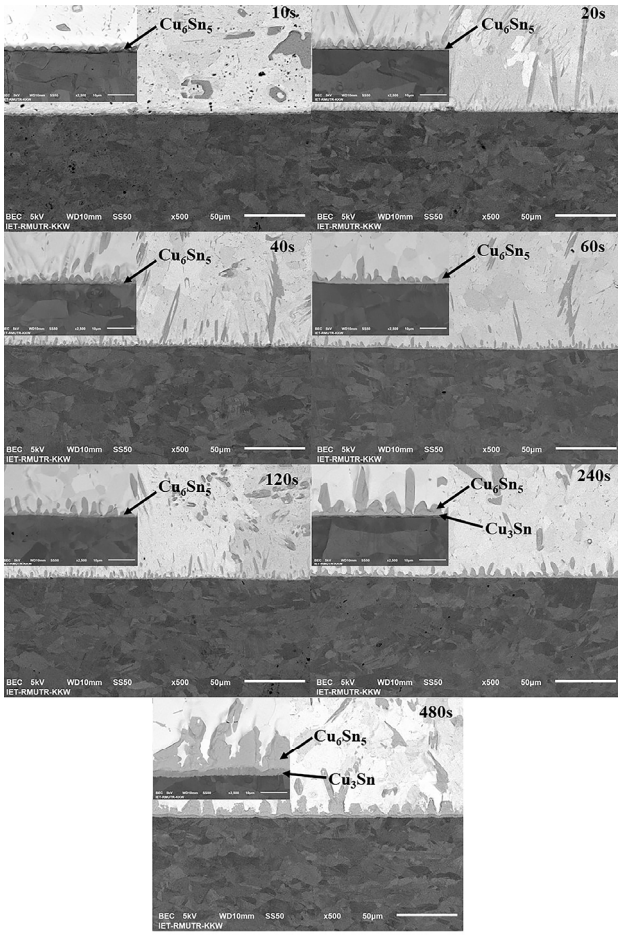

Fig. 4. SEM microstructure with soldering time.

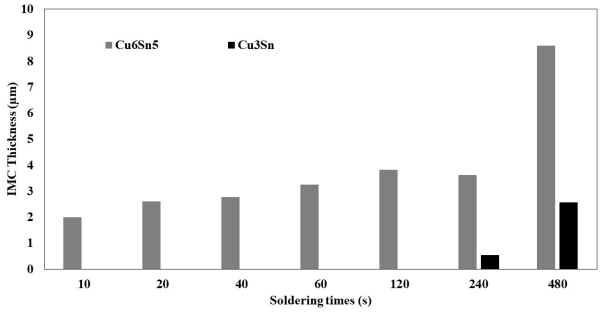

Fig. 5. IMC thickness with soldering time.

Fig. 6 shows the phase fraction of Cu_6Sn_5 in the Sn matrix determined by advanced phase analysis, with results expressed as phase fraction area. Fig. 7 illustrates the percentage of Cu_6Sn_5 phase in the solder for all time points. Volume fraction of Cu_6Sn_5 phase in the solder matrix increased with soldering time due to increased nucleation during solder solidification.

Table 1. Composition of intermetallic phases.

Phase	Cu (at.%)	Sn (at.%)	Ref.
Cu_6Sn_5	51.11-52.77	Balanced	This study
Cu_3Sn	70.74-73.38	Balanced	This study
Cu_6Sn_5	53.30	44.70	[18]
Cu_3Sn	74.90	25.1	[18]

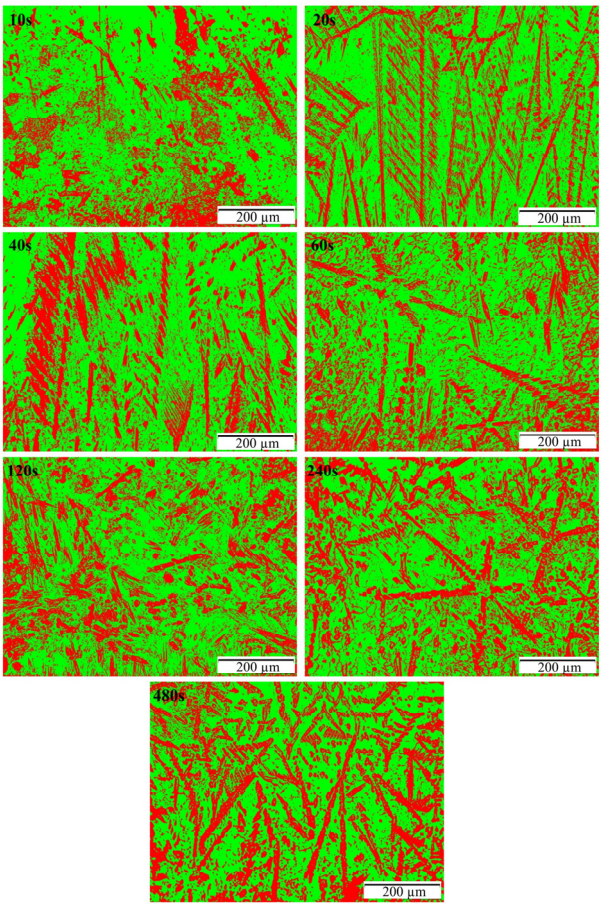

Fig. 6. Phase fraction of Cu_6Sn_5 with soldering time.

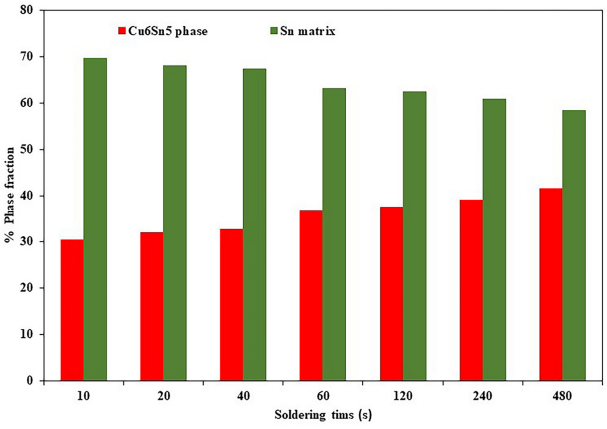

Fig. 7. Percentage of Cu_6Sn_5 phase in Sn matrix.

Thickness of the intermetallic phase was elucidated by equations (2) and (3).

$$Y = kt^n \quad (2)$$

$$Log\ Y = log\ k + n\ log\ t \quad (3)$$

where Y is the thickness of the intermetallic phase, k is the intermetallic growth rate constant, t is the reflow soldering time, and n is the time exponent.

The value of n was determined from the slope of plot between log Y with log t. It is well known that volume of n has a significant effect on the growth rate of the intermetallic phase. When n=1/3, the intermetallic phase growth follows the grain boundary diffusion-controlled; when n=1/2, the intermetallic phase growth follows the volume diffusion-controlled; when n=1, the intermetallic phase growth follows the reaction-controlled [21-23]. The time exponent values for Cu_6Sn_5 and Cu_3Sn phases were 0.083 and 0.682, respectively. This phenomenon can be explained in terms of the growth rate controlled by grain boundary diffusion and volume diffusion-controlled for Cu_6Sn_5 and Cu_3Sn phases, respectively. In summary, relationship between the contact angle and intermetallic phase formation resulted from increase of the intermetallic phase during soldering in response to decreasing contact angle.

4. Conclusion

Influence of soldering time on contact angle and intermetallic phase formation during soldering were investigated. Insignificant change in grain size of copper substrate was recorded as soldering time increased. However, increasing soldering time significantly altered contact angle of the solder and intermetallic phases. Cu_6Sn_5 and Cu_3Sn phases were found at the interface zone. The Cu_3Sn phase only formed when the reflow time became very long. Total thickness of the intermetallic phase increased with post-soldering time, implying that the mechanisms were controlled via grain boundary and volume diffusion. Thus, soldering time was fundamental for controlling wettability and intermetallic phase formation within the soldering process, and necessary to determine a comprehensive approach to develop overall performance of high-temperature solders.

Acknowledgements:

This research was financially supported by Faculty of Engineering, King Mongkut's Institute of Technology Ladkrabang (KMITL).

References

1. D.R. Reinosa, *IEEE International Conference on Test* (2005)
2. S. Prabhu, K.N, Adv. Colloid. Interface. Sci. **166**, 87–118 (2011)
3. J. Watson, G. Castro. Analog Dialogue 46-04 (2012)
4. J. Liang, N. Dariavach, P. Callahan, D. Shangguan, Mater Trans. **47**, 317–325 (2006)
5. C. Lei, H. Huang, Y. Huang, Z. Cheng, S. Tang, Y. Du, Powder Tech. **301**, 356–359 (2016)
6. L. Zang, Z. Yuan, H. Zhao, X. Zhang, Mater Lett. **63**, 2067–2069 (2009)
7. Q. Zeng, J. Guo1, X. Gu, X. Zhao, X. Liu, J. Mater. Sci. Technol. **26**, 156–162 (2010)
8. H. Wang, F. Wang, F. Gao, X. Ma, Y. Qian, J. Alloy Comp. **433,** 302–305 (2007)
9. D.Q. Yu, H.P. Xie, L. Wang, J. Alloy Comp. **385**, 119–125 (2004)
10. M. F. Arenas, V. L. Acoff, J. Electron Mater. **33**, 1452–1458 (2004)
11. T. Novak, J. Stary, F. Steiner, P. Stejskal, *Electroscope, Conference EDS* (2009)
12. Y.Y. Chen, J.G. Duh, J. Mater Sci. **11**, 279–283 (2000)
13. L. Lin, S. Hui, G. Lu, S-L. Wang, X-D. Wang, D.J. Lee, Chem Eng Sci. **174**, 127–135 (2017)
14. L. Zang, Z. Yuan, H. Xu, B. Xu, Appl Surf Sci. **257**, 4877–4884 (2011)
15. X. Wang, J. Han, F. Guo, L. Ma, Y. Wang, *International Conference on Electronic Packaging Technology* (2017)
16. C. Yu, H. Lu, S. Li, J. Alloy Comp. **460**, 594–598 (2008)
17. Y. Wang, D.T. Chu, K.N. Tu, *IEEE Electronic Components and Technology Conference*, 439–446 (2016)
18. Z. Yin, F. Sun, M. Guo, Mater Lett. **215,** 207–210 (2018)
19. S. Fürtauer, D. Li, D. Cupid, H. Flandorfer, Intermetallics, **34**, 142–147 (2013)
20. N. Mookam, K. Kanlayasiri, *ICMM, international Conference on Mechatronics and Manufacturing* (2018)
21. M. Schaefer, R.A. Fournelle, J. Liang. J. Electron Mater. **27**, 1167–1176 (1998)
22. X. Deng, G. Piotrowski, J.J. Williams, N. Chawlai, J. Electron Mater. **32**, 1403–1413 (2003)
23. Y. Yao, J. Zhou, F. Xue, X. Chen, J. Alloy Comp. **682**, 627–633 (2016)